

# Charge and orbital ordering in $\text{Pr}_{0.5}\text{Ca}_{0.5}\text{MnO}_3$ studied by $^{17}\text{O}$ NMR

A. Yakubovskii,<sup>1,2</sup> A. Trokiner,<sup>2</sup> S. Verkhovskii,<sup>3</sup> A. Gerashenko,<sup>3</sup> and D. Khomskii<sup>4</sup>

<sup>1</sup>Russian Research Centre "Kurchatov Institute," Moscow, 123182 Russia

<sup>2</sup>Laboratoire de Physique du Solide, Ecole Supérieure de Physique et de Chimie Industrielles, Paris, France

<sup>3</sup>Institute of Metal Physics, Russian Academy of Sciences, 620219 Ekaterinburg, Russia

<sup>4</sup>Laboratory of Solid State Physics, Groningen University, Netherlands

(Received 8 September 2002; published 26 February 2003)

The charge and orbital ordering in  $\text{Pr}_{0.5}\text{Ca}_{0.5}\text{MnO}_3$  is studied for the first time by  $^{17}\text{O}$  NMR. This local probe is sensitive to spin, charge, and orbital correlations. Two transitions exist in this system: the charge and orbital ordering at  $T_{CO} = 225$  K and the antiferromagnetic (AF) transition at  $T_N = 170$  K. Both are clearly seen in the NMR spectra measured in a magnetic field of 7 T. Above  $T_{CO}$  there exists only one NMR line with a large isotropic shift, whose temperature dependence is in accordance with the presence of ferromagnetic (FM) correlations. This line splits into two parts below  $T_{CO}$ , which are attributed to different types of oxygen in the charge-/orbital ordered state. The interplay of FM and AF spin correlations of Mn ions in the charge-ordered state of  $\text{Pr}_{0.5}\text{Ca}_{0.5}\text{MnO}_3$  is considered in terms of the hole hopping motion that slows down with decreasing temperature. The developing fine structure of the spectra evidences that there still exist charge-disordered regions at  $T_{CO} > T > T_N$  and that the static ( $\tau > 10^{-6}$  s) orbital order is established only on approaching  $T_N$ . The charge-exchange (CE) type magnetic correlations develop gradually below  $T_{CO}$ , so that at first the AF correlations between checkerboard  $ab$  layers appear, and only at lower temperature do CE correlations within the  $ab$  planes appear.

DOI: 10.1103/PhysRevB.67.064414

PACS number(s): 75.30.Et, 76.60.Cq

## I. INTRODUCTION

Charge-ordering phenomena in hole-doped  $R_{1-x}A_x\text{MnO}_3$  ( $R$  is a trivalent rare-earth ion and  $A$  is a divalent alkaline-earth ion) have been a subject of extensive studies due to intriguing interplay of the charge, orbital, and spin degrees of freedom. The charge-ordered (CO) state is formed due to localization of the mobile  $e_g$  holes.

Above  $T_{CO}$  the  $e_g$  holes provide ferromagnetic (FM) correlations between electron spins of neighboring manganese ions through the double-exchange (DE) mechanism proposed by Zener.<sup>1</sup>  $\text{Pr}_{1-x}\text{Ca}_x\text{MnO}_3$  ( $0.3 \leq x \leq 0.75$ ) oxides are the most suitable for investigation of the CO state since the onsets of the charge ( $T_{CO}$ ) and spin ( $T_N$ ) order are well separated in temperature. This doped oxide has an orthorhombic structure (space group  $Pbnm$ ) in a wide temperature and magnetic-field ( $< 20$  T) range. It remains in the semiconducting state with no admixture of the FM metal phase, as opposed to  $\text{Pr}_{1-x}\text{Sr}_x\text{MnO}_3$ ,  $\text{La}_{1-x}\text{Ca}_x\text{MnO}_3$ , and  $\text{La}_{1-x}\text{Sr}_x\text{MnO}_3$ .<sup>2,3</sup> In the CO structure of  $\text{Pr}_{1-x}\text{Ca}_x\text{MnO}_3$  with  $x \sim 0.5$  the in-plane pattern of  $\text{Mn}^{3+}$  and  $\text{Mn}^{4+}$  ions may be represented as a checkerboard related to the corresponding  $t_g^3 e_g^1$  and  $t_g^3$  electronic configurations of Mn (Fig. 1). The lobes of a certain number of occupied  $e_g$  orbitals are ordered in the direction of the  $\text{Mn}^{3+}-\text{O}-\text{Mn}^{4+}$  bond to maximize DE coupling, whereas the antiferromagnetic (AF) superexchange  $t_{2g}-t_{2g}$  coupling is a dominating magnetic interaction for  $\text{Mn}^{4+}$  and  $\text{Mn}^{3+}$  whose  $e_g$  lobes are aligned perpendicular to the  $\text{Mn}^{3+}-\text{O}-\text{Mn}^{4+}$  bond. At  $x \sim 0.5$  the competition of these exchange couplings results in the AF spin ordering of a charge-exchange (CE) type with  $T_N < T_{CO}$ . The associated Jahn-Teller (JT) distortions of  $\text{MnO}_6$  octahedra double the unit cell along the  $b$  axis of the orthorhombic ( $Pbnm$ ) lattice. The ideal CE-type charge/orbital

order implies a FM zigzag arrangement of the ordered  $e_g(3x^2-r^2)$  and  $e_g(3y^2-r^2)$  orbitals of  $\text{Mn}^{3+}$  ions in the  $ab$  plane. The neighboring zigzags are antiferromagnetically coupled, and the ordering in the  $c$  direction is also antiferromagnetic.

Recent resonant x-ray scattering,<sup>4</sup> electron microscopy,<sup>5</sup> and neutron-diffraction<sup>6,7</sup> studies of  $\text{Pr}_{0.5}\text{Ca}_{0.5}\text{MnO}_3$  have shown that the orbital order (OO) below  $T_N = 170$  K results in an orbital domain state commensurate with the lattice. This commensurate OO becomes metastable above  $T_N$ . Its melting is observed in diffraction studies as a commensurate-incommensurate (C-IC) transition at  $T_{C-IC} \sim (180-200)$  K  $> T_N$ . With further increase of temperature the partial orbital disorder turns on the FM spin fluctuations which become

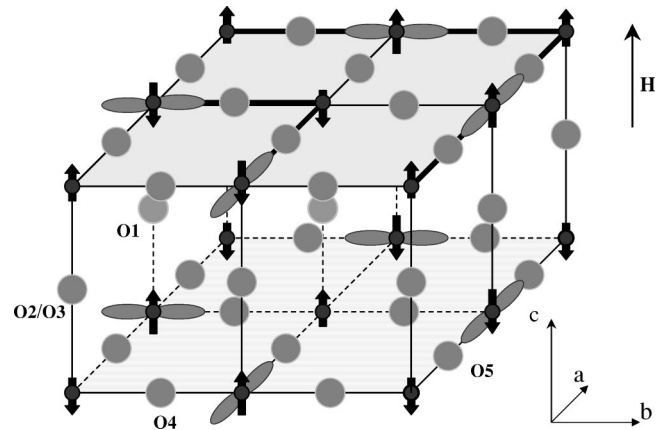


FIG. 1. Charge- and orbital ordered  $\text{Pr}_{0.5}\text{Ca}_{0.5}\text{MnO}_3$  with CE-type magnetic structure: (●)  $\text{Mn}^{4+}$  ions; (○)  $\text{Mn}^{3+}$  ions with occupied  $e_g$  orbitals; (●) oxygen ions (O1–O5). The CE type of spin correlation in the charge-ordered paramagnetic phase is shown by arrows directed up/down relative to the applied magnetic field  $\mathbf{H} \parallel \mathbf{c}$ .

dominating near  $T_{CO} \approx 250$  K.<sup>8</sup> The C-IC transition was considered in terms of the  $e_g$ -orbital polarization soft mode. The  $e_g$  orbital completely polarized along the Mn-O bond corresponds to the amplitude of the wave at a given  $\text{Mn}^{3+}$  ion<sup>6</sup> and its wave vector  $\mathbf{q} = \{0, 1/2 - \epsilon, 0\}$  was considered as the order parameter of the transition.

Further discussion of the CO state requires more detailed microscopic data related to the distribution of spin density and to its dynamic regime in the CO state of manganite. Studies of spatial fluctuations of charge/orbital order with diffraction experiments<sup>6,7</sup> are restricted to short correlation times  $\tau_c < 10^{-12}$  s, whereas NMR experiments enable studying time-dependent spin fluctuations at a much longer  $\tau_c$ .

In this work we have studied the spin correlations of the neighboring Mn ions developed in the paramagnetic charge-ordered (PM CO) state of  $\text{Pr}_{0.5}\text{Ca}_{0.5}\text{MnO}_3$  by measuring the  $^{17}\text{O}$  NMR spectra. Oxygen atoms being placed between two Mn ions bring valuable information about the spin/orbital configuration of the nearest Mn ions. As expected the nuclear spin of oxygen ( $^{17}\text{I} = 5/2$ ) probes its magnetic state through the dipolar and transferred hyperfine magnetic fields that depend on the spin/orbital configuration of the neighboring Mn ions.<sup>9</sup> The  $^{55}\text{Mn}$  nucleus is a less suitable NMR probe for this task for the following reasons. First, the NMR spectrum of the  $\text{Mn}^{4+}$  ion ( $t_g^3$ -electron configuration) is available only at low temperatures in the metastable CO AF phase. On the other hand, NMR of  $\text{Mn}^{3+}$  ( $t_g^3 e_g^1$ ) is hard to detect due to the extremely high nuclear spin-spin relaxation rate apparently controlled by abnormal the low-frequency spin dynamic of the localized  $e_g$  electrons.

This  $^{17}\text{O}$  NMR report is focused on the study of the development of the charge/orbital ordering in  $\text{Pr}_{0.5}\text{Ca}_{0.5}\text{MnO}_3$ . The main result is that in  $\text{Pr}_{0.5}\text{Ca}_{0.5}\text{MnO}_3$  the CE-type magnetic correlations develop gradually below  $T_{CO}$ : first those between  $ab$  layers arise and only at lower temperature do the correlations within  $ab$  planes appear. The static ( $\tau_c > 10^{-6}$  s) orbital order is established only on approaching  $T_N$ . Recently<sup>21</sup> an alternative picture of ordering was suggested for  $\text{Pr}_{0.6}\text{Ca}_{0.4}\text{MnO}_3$ : from the single-crystal structural data the authors<sup>21</sup> concluded that instead of the conventional site-centered charge ordering of the checkerboard type, there appears a bond-centered superstructure (Zener polarons) with essentially equivalent Mn ions. Most of the existing data for half-doped manganites support the usual CE type of ordering<sup>22,23</sup> and in the interpretation of our data we use this picture; our data are yet not sufficient to discriminate between these two models (in both of them there will be several inequivalent oxygen sites, with rather similar properties). Nevertheless this question definitely deserves further study.

## II. EXPERIMENT

We used a powder sample of  $\text{Pr}_{0.5}\text{Ca}_{0.5}\text{MnO}_3$  prepared by traditional ceramic technology. The powder was enriched with a  $^{17}\text{O}$  isotope up to  $\approx 25\%$ . The single-phase nature of the enriched sample was confirmed by the x-ray-diffraction and Raman-scattering studies at room temperature.

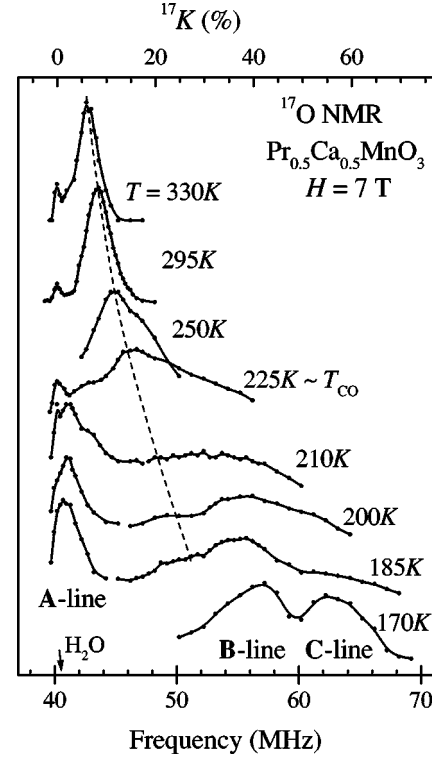


FIG. 2.  $^{17}\text{O}$  NMR spectra measured at  $H = 7$  T in the paramagnetic state of  $\text{Pr}_{0.5}\text{Ca}_{0.5}\text{MnO}_3$ . The dashed line represents the fitting curve of the line peak shift by the expression  $K_0 + a/(T - \theta)$  for spectra measured above  $T_{CO}$ .

$^{17}\text{O}$  NMR measurements were carried out on a phase-coherent NMR pulse Bruker spectrometer over the temperature range of 80–330 K in magnetic field of 7 T. In this field the onset of the CO and AF spin ordering was found to shift slightly down to  $T_{CO} \approx 225$  K and  $T_N \approx 170$  K compared to reported data at zero field and in accordance with the  $H$  dependence of  $T_{CO}$  reported in Ref. 3. NMR spectra were obtained for a loosely packed powder sample with point-by-point frequency sweep measurements, with the intensity of the spin-echo signal formed with the pulse sequence  $(\pi/2) - \tau_{del} - (\pi/2)$  echo measured. The width of the  $\pi/2$ -exciting pulse was  $t_p = (2 - 4.5) \mu\text{s}$  and the distance between pulses varied in the range of  $\tau_{del} = (40 - 80) \mu\text{s}$ . For each frequency, the amplitude of the exciting rf pulse was adjusted in order to optimize the echo signal intensity while keeping the pulse duration fixed. All the echo intensities were corrected to  $\tau_{del} \approx 0$  by measuring the rate of echo decay at different frequencies of the broad spectrum. All the spectra for  $T < T_{CO}$  were measured during cooling down from room temperature to avoid the hysteresis uncertainties. The  $^{17}\text{O}$  NMR signal in  $\text{H}_2\text{O}$  was used as a frequency reference to determine the shift of NMR line in our sample.

## III. RESULTS AND DISCUSSION

### A. The charge-disordered paramagnetic state

Figure 2 shows the  $^{17}\text{O}$  NMR spectra of  $\text{Pr}_{0.5}\text{Ca}_{0.5}\text{MnO}_3$  measured in the PM state. In the charge-disorder paramag-

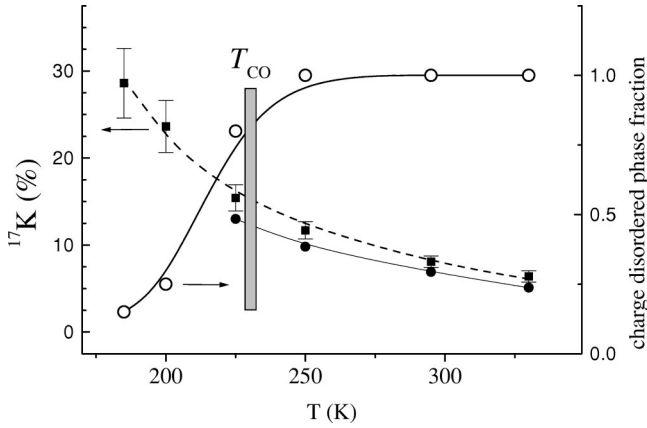


FIG. 3. (a) The line peak shift  $K$  (solid squares) and  $^{17}K_{\perp}$  (solid circles) vs  $T$  plot. The dashed curve is the fit of  $K$  data by the expression  $K_0 + a/(T - \theta)$  with  $K_0 = -1.0(6)\%$  and  $\theta = 130(10)$  K for spectra measured above  $T_{CO}$ ; the solid line represents the fitting curve of the line peak shift by the expression  $K_0 + a/(T - \theta)$ . (b) Relative  $^{17}\text{O}$  NMR line intensity of oxygens in the charge-disordered regions of the PM phase.

netic (CD PM) state for  $T > T_{CO} \approx 225$  K the main signal ( $\sim 95\%$ ) in the spectrum is a rather asymmetric line. It has a positive and extremely large magnetic shift exceeding 6% even at the highest measured temperature,  $T = 330$  K, with respect to those observed in nonmagnetic compounds. An additional line of small intensity ( $\sim 5\%$ ) is present at zero NMR shift. It is supposed to originate from a small amount of the Ca-based oxides, which arise as spurious precipitations during the solid-state reaction synthesis. It's well known that a small concentration of spurious phase formed with light atoms such as Ca is hard to detect by x ray.

Let us now consider the quadrupolar and magnetic shift interactions of the oxygen nuclear spin with its environment. The oxygen atoms are located at the corners of octahedra with Mn at the center. The noncubic local symmetry of oxygen sites leads to the interaction of the  $^{17}\text{O}$  electric quadrupole moment ( $eQ$ ) with electric-field gradient ( $eV_{ZZ}$ ). The resulting  $^{17}\text{O}$  NMR spectrum is expected to split into  $2I + 1$  lines separated by the quadrupole frequency  $\nu_Q = (3e^2Q)/(2I(2I - 1)\hbar V_{ZZ})$  at  $\mathbf{H} \parallel O_z$ . Experimentally this characteristic first-order quadrupole splitting has never been observed. It shows that  $^{17}\nu_Q$  does not exceed the NMR linewidth measured at  $T = 330$  K, i.e.,  $\nu_Q < 1.4$  MHz in agreement with Ref. 10. Thus the quadrupolar interaction will only provide broadening effects on the observed pattern of NMR spectra, but these quadrupolar effects are small compared to the magnetic interaction effects (see below).

The powder pattern spectrum of the  $\text{Pr}_{0.5}\text{Ca}_{0.5}\text{MnO}_3$  main line in the CD PM state may be described assuming an axial symmetry of the magnetic shift tensor  $\{K_{\perp}, K_{\perp}, K_{\parallel}\}$ . The subscript “ $\perp$ ” or “ $\parallel$ ” refers to the shift component  $K_{\alpha}$  of oxygen with the Mn-O bond directed perpendicular or parallel to the external magnetic field  $H_0$ , respectively. The analysis of the line leads to  $K_{\perp} = 7.0\%$  and  $K_{\parallel} = 11.5\%$  at  $T = 295$  K. The thermal variation of the shift is shown in Fig. 3. With decreasing temperature the peak of the line is further shifted following the Curie-Weiss law with  $K = K_0 + a/(T$

$-\theta$ ). The corresponding fit curve drawn by a dashed line in Figs. 2 and 3 results in  $K_0 = -1.0(6)\%$  and  $\theta = 130(20)$  K. A close value of  $\theta \sim 150$  K is obtained by fitting the magnetic-susceptibility ( $\chi$ ) data measured in the range of  $T = 250 \div 300$  K in Ref. 6. The positive value of  $\theta$  evidences that FM spin correlations between neighboring Mn are the dominating ones in the CD PM state above  $T_{CO}$ . A similar conclusion about the prevalence of the FM spin correlations between Mn ions in the CD PM phase was inferred from the  $^{139}\text{La}$  NMR line shift in  $\text{La}_{0.5}\text{Ca}_{0.5}\text{MnO}_3$ , which becomes a FM metal in the field of 4 T below  $T \approx 220$  K.<sup>11</sup>

The slope of the  $K$  vs  $\chi$  plot corresponds to the local magnetic field  $H_{loc} = \mu_B \Delta K / \Delta \chi \approx 1 \times 10^4$  Oe/ $\mu_B$  (the  $\chi$  data are taken from Fig. 4 in Ref. 6). It exceeds the magnitude of the classic dipolar field ( $H_{dip}$ ) induced at the oxygen ion by the magnetic moments of the neighboring Mn ions:

$$H_{dip} = \frac{2g_e\mu_B\langle s_z(\text{Mn}) \rangle}{r_{\text{Mn-O}}^3} = \frac{2\chi H}{r_{\text{Mn-O}}^3}. \quad (1)$$

At room temperature  $H_{dip}$  may be estimated as  $H_{dip} \approx 1200$  Oe where  $\chi$  is defined per spin from Ref. 6. The corresponding estimated anisotropic contribution to the total NMR line shift  $\{-0.8\%, -0.8\%, 1.6\%\}$  is much less than the experimental value. Thus we assume that the classic dipole interaction of the  $^{17}\text{O}$  nucleus with effective magnetic moments  $2g_e\mu_B\langle s_z(\text{Mn}) \rangle$  of the nearest Mn has no strong influence on the total shape of the spectrum.

The most probable origin of the observed giant isotropic magnetic shift  $K_{iso} = (2K_{\perp} + K_{\parallel})/3$  is the Fermi-contact interaction of the nuclear spin  $^{17}I$  with the transferred  $s$ -spin density of electrons participating both in the Mn-O-Mn bonding and in superexchange coupling of the neighboring Mn,

$$K_{iso} = \frac{8\pi}{3} g_e\mu_B |\phi_{2s}(0)|^2 f_s \langle s_z(\text{Mn}) \rangle \\ = \frac{1}{^{17}\gamma\hbar} a(2s) f_s \langle s_z(\text{Mn}) \rangle. \quad (2)$$

Here  $g_e\mu_B\langle s_z(\text{Mn}) \rangle = \chi H$ ,  $a(2s) = ^{17}\gamma\hbar H_{FC}(2s) = 0.15 \text{ cm}^{-1}$  is the isotropic hyperfine coupling constant for the oxygen ion.<sup>12,13</sup>  $H_{FC}$  is the corresponding hyperfine magnetic field due to the Fermi-contact interaction with electron located on the  $2s$  orbital with wave function  $\psi_{2s}(r)$ . Following Refs. 14 and 9, the corresponding isotropic spin density transferred at the oxygen ion from neighboring Mn ions may be defined in terms of the factor  $f_s = H_{loc,iso}/2H_{FC}(2s)$ . This quantity estimated from Eq. (2) results in a rather large magnitude of the effective fractional occupancy of  $O(2s)$  orbitals by unpaired spins. We found  $f_s = 0.01$  for the insulating PM state of  $\text{Pr}_{0.5}\text{Ca}_{0.5}\text{MnO}_3$ . For comparison the local-density approximation +  $U$  band-structure calculation results in  $f_s = 0.003 - 0.007$  for the FM ordered state of  $\text{LaMnO}_3$ .<sup>15</sup>

Another possible isotropic hyperfine interaction is the core-polarization term which provides  $H_{loc} \approx 3 \times 10^4$  Oe,<sup>16</sup> when assuming that the doped electron is fully localized within the oxygen  $2p$  orbital. But this is not the case above



$T_{CO}$  in  $\text{Pr}_{0.5}\text{Ca}_{0.5}\text{MnO}_3$ . Thus this interaction may be neglected for the light oxygen atom.

The noncubic local symmetry of oxygen sites gives rise to an anisotropic part of the magnetic shift tensor  $K_{ax} = (K_{\parallel} - K_{\perp})/3$ . The most reasonable contribution to  $K_{ax}$  is the magnetic dipole-dipole hyperfine interaction of  $^{17}\text{O}$  with electrons on  $2p_{\sigma\pi}$  orbitals, whose “up-” and “down-” spin occupancies become different through the polarizing interactions with neighboring manganese. The corresponding magnetic shift tensor  $K_{dip}$  may be expressed through the fractional spin-density transfer  $f_{\alpha}\langle s_z(\text{Mn}) \rangle$  on the O  $2p_{\alpha}$  orbital from the paramagnetic neighboring Mn ion<sup>9</sup> as

$$K_{\parallel}(2p_{\sigma}) = -2K_{\perp}(2p_{\sigma}) = \frac{4}{5}\langle r^{-3} \rangle_{2p} f_{\sigma} \chi(\text{Mn}), \quad (3)$$

with  $K_{\parallel}(2p_{\sigma})$  [ $K_{\perp}(2p_{\sigma})$ ] defined for  $H_0$  parallel (perpendicular) to the Mn-O bond, respectively. The resulting dipolar contribution to  $K_{ax}$  is thus determined by the difference of transferred spin density  $(f_{\sigma} - f_{\pi})\langle s_z(\text{Mn}) \rangle$  for different O  $2p$  orbitals from the neighboring Mn ion:<sup>9</sup>

$$K_{ax} = \frac{2}{5}\langle r^{-3} \rangle_{2p} (f_{\sigma} - f_{\pi}) \chi(\text{Mn}). \quad (4)$$

Taking  $\langle r^{-3} \rangle_{2p} = 4.97$  a.u. (Ref. 13) for the neutral oxygen atom we obtain a rather large positive value  $(f_{\sigma} - f_{\pi}) \approx 0.04$ . The direct observation of the positive value of  $(f_{\sigma} - f_{\pi})$  proves that the  $p_{\sigma}$  orbital directed along the Mn-O bond is more polarized than the two other  $p_{\pi}$  orbitals.

We showed before that the  $^{17}\text{O}$  NMR line position in the CD PM state is mainly determined by the isotropic transferred hyperfine coupling, arising from the hybridization of Mn( $3d$ ) and O( $2s$ ) orbitals. In the ideal  $Pbnm$  structure there is no overlap of Mn( $t_{2g}$ )–O( $2s$ ) orbitals due to their orthogonality, while  $e_g$  orbitals of Mn have a rather strong overlap with the  $s$  orbital of neighboring oxygen as shown in Fig. 1. Hereafter we restrict ourselves to the effects of overlap and covalency between Mn( $e_g$ ) and O( $2s$ ) orbitals.

### B. The charge-ordered paramagnetic state

Just below  $T_{CO}$  the  $^{17}\text{O}$  NMR spectrum is substantially broadened. It splits into two parts as shown in Fig. 2. The low-frequency spectrum in the range of  $K = (-2 \div +10)\%$  is asymmetric ( $A$  line). Its width decreases gradually as the temperature approaches  $T_N$ . The high-frequency spectrum is approximately twice larger in intensity and forms a rather complicated pattern whose center of gravity is shifted to extremely large positive  $K > 20\%$ . At  $T = 170 \text{ K} \approx T_N$  it splits into two broad lines ( $B$  and  $C$  lines) of about equal intensity and peak at  $K_B \approx 40\%$  and  $K_C \approx 55\%$ , respectively.

According to x-ray and neutron-diffraction studies,<sup>6</sup> the charge order and OO of the CE type become commensurate in the CO PM phase only near  $T_N$ . If the domain structure of the OO (Refs. 4 and 6) is ignored, one finds four groups of the oxygen atoms differentiated by the charge and/or by the direction of occupied  $e_g$  orbital of the nearest-neighboring Mn ions. The first and the second groups are formed by apical oxygen located between two  $\text{Mn}^{3+}$  ions (O1 site,

shown in Fig. 1) or between  $\text{Mn}^{4+}$  (O2/O3 sites), respectively. Note that the  $s_z$  projections of electron spins are AF, correlated for neighboring Mn from adjacent  $ab$  planes. A third group is formed by oxygen (O4) in the  $ab$  plane, which participates in the AF coupling of neighboring  $\text{Mn}^{4+}$ ,  $\text{Mn}^{3+}$  from adjacent zigzags. The last group (O5) is formed by oxygen in the  $ab$  plane located between two FM coupled  $\text{Mn}^{4+}$  and  $\text{Mn}^{3+}$  ions inside a zigzag. The concentration of each type of oxygen atom obeys the “structural” ratio 1:1:2:2.

In order to assign  $A$ – $C$  lines measured in the CO PM phase we analyze first the spectra near  $T_N$  with resolved structure. We compare the “structural” ratio with the experimental “NMR line intensity” ratio, which is close to 2:2:2. We also take into account that the local magnetic fields at different oxygen sites are formed through the Mn-O-Mn exchange interactions which are short range in space. In the CO PM phase the effective magnetic moment of Mn (shown in Fig. 1 by arrows) is defined by its projection  $g_e \mu_B \langle s_z \rangle$  on the direction of the external magnetic field. In turn it controls the sign of the corresponding  $^{17}\text{O}$  NMR shift contributed by each of the two neighboring Mn.

The  $A$  line is attributed to the apical (O1, and O2/O3) sites, whereas the  $B$  and  $C$  lines to the in-plane ones. The magnetic shift of the  $A$  line is small, and the local field at the corresponding  $^{17}\text{O}$  is comparable in magnitude to the classic dipolar field estimated above (1). At these apical sites the hyperfine magnetic shifts (2–4) are greatly reduced since both neighboring Mn ions are in the same valence state and their effective magnetic moments  $g_e \mu_B \langle s_z \rangle$  are AF, correlated in the CO PM phase of the CE type.

Let us now consider the high-frequency part of the spectra. The  $C$  line demonstrating the largest positive shift may be attributed to oxygen positioned in O5 sites, whereas the  $B$  line is presumably due to oxygen located in O4 sites. Indeed for oxygen in the O5 site the transferred  $s$ -wave spin density is maximal since within the zigzag the lobe of the partially occupied  $e_g(m_l=0)$  orbital of the  $\text{Mn}^{3+}$  ion points toward the neighboring oxygen. Furthermore the two neighboring Mn ions are ferromagnetically correlated. For O4 we definitely expect a rather large transferred hyperfine field for the following reason. Although the spins of Mn in adjacent zigzags are antiparallel, the O4 oxygen is “sandwiched” between  $\text{Mn}^{3+}$  and  $\text{Mn}^{4+}$  ions with different spin values and different orbital occupations, i.e., with different covalency, so that the transferred polarization from these two Mn ions should not compensate as they do for the apical oxygen (O1, O2/O3). This should again result in a substantial shift, although smaller than for O5. Moreover the transferred  $s$ -wave polarization from the  $\text{Mn}^{4+}$  ion is expected to be negative due to effects of covalent mixing with the empty  $e_g$  orbitals.<sup>17</sup> As reviewed in Ref. 18 the charge transfer from the occupied O  $2s$  orbital to the empty  $e_g$  orbital is spin dependent. It is regulated by the intra-atomic exchange coupling with electrons on  $t_g$  orbitals.

Thus in the CO PM phase the static  $s$ -wave polarization is directed along  $\mathbf{H}$ , and the isotropic shift at the O5 site may be expressed similarly to Eq. (2) through the corresponding

transferred spin densities  $f_{s,3+}\langle s_z(\text{Mn}^{3+}) \rangle$  or  $f_{s,4+}\langle s_z(\text{Mn}^{4+}) \rangle$  of the neighboring Mn (with  $f_{s,3+} > 0$  and  $f_{s,4+} < 0$ ):

$$K_{iso}(\text{O5}) = \frac{8\pi}{3} g_e \mu_B |\psi_{2s}(0)|^2 \{ f_{s,3+} \langle s_z(\text{Mn}^{3+}) \rangle + f_{s,4+} \langle s_z(\text{Mn}^{4+}) \rangle \}. \quad (5)$$

The effective magnetic moments of neighboring Mn from adjacent zigzags are antiferromagnetically correlated and we obtain for  $K_{iso}(\text{O4})$  the following expression:

$$K_{iso}(\text{O4}) = \frac{8\pi}{3} g_e \mu_B |\psi_{2s}(0)|^2 \{ 0.25 f_{s,3+} \langle s_z(\text{Mn}^{3+}) \rangle - f_{s,4+} \langle s_z(\text{Mn}^{4+}) \rangle \}. \quad (6)$$

The signs “+”/“−” in Eqs. (5) and (6) take into account the fact that FM/AF spin correlations of the neighboring  $\text{Mn}^{3+}$  and  $\text{Mn}^{4+}$  ions are considered as static in the time interval which is much longer than the inverse splitting of the  $B$  and  $C$  lines ( $\sim 10^{-8}$  s) of the spectrum at  $T = 170$  K  $\approx T_N$ , when charge order and OO are completely formed in the PM state. This agrees with the fact that the  $\text{O}(2s)$  polarization is provided predominantly by the  $\sigma$  overlap with the  $e_g$  orbitals of Mn, and Pauli blocking of part of the  $e_g$  orbitals in  $\text{Mn}^{3+}$  gives stronger polarization than in the case of  $\text{Mn}^{4+}$ , where both  $2s\uparrow$  and  $2s\downarrow$  electrons of O2 may virtually hop to  $\text{Mn}^{4+}$  so that the net oxygen polarization due to covalency with  $\text{Mn}^{4+}$  will be smaller, than for the  $\text{Mn}^{3+}$  neighbor, and negative. For a crude estimate of the transferred  $s$ -spin density we have assumed in Eqs. (5) and (6) that the  $\sigma$  overlap of the  $e_g(m_l=0)$  orbital of  $\text{Mn}^{3+}$  with the  $2s$  orbital of O5 in zigzag of the CE-type of charge- and orbital ordered phases is twice as large as the overlap with the corresponding  $2s$  orbital of oxygen (O4) located between the neighboring zigzags in the  $ab$  plane. (Of course under detailed consideration it should depend on interatomic distance and on the bending of the  $\text{Mn}^{3+}-\text{O}$  bond in the tilted and JT distorted  $\text{MnO}_6$  octahedra.) Inserting the value of the peak position of the  $B$  line ( $K_{iso}=40\%$ ) and  $C$  line ( $K_{iso}=55\%$ ) into expressions (6) and (5), respectively we get that the transferred  $s$ -wave polarization from the  $\text{Mn}^{3+}$  ion is positive and its absolute value exceeds by about four times the corresponding negative polarization transferred from  $\text{Mn}^{4+}$   $|f_{s,4+}\langle s_z(\text{Mn}^{4+}) \rangle|$ .

The large difference in spin densities transferred from the  $\text{Mn}^{3+}/\text{Mn}^{4+}$  ions indicates a substantial delocalization of the “ $e_g$  hole” within the hybridized  $e_g(\text{Mn}^{3+})-2p_\sigma(\text{O})$  orbital.<sup>19</sup> It shows that a pure ionic approach where the  $e_g$  hole is completely localized at the  $\text{Mn}^{3+}$  ion is a very rough approximation to describe in detail the charge order and OO in doped manganite.

In the given interpretation of the  $^{17}\text{O}$  NMR spectra we follow to the picture of the conventional site-centered charge ordering. Regarding our data to another scenario of

charge ordering of the bond-ordered structure of Zener polarons as suggested by Daoud-Aladine *et al.*,<sup>21</sup> we can say the following:

In both models we expect antiferromagnetic correlations between  $ab$  layers (if the charge ordering between layers is in phase, which seems to be the case in both models of charge ordering). Consequently, we should expect a signal due the apical oxygens at zero NMR shift (line A) in both models. As explained above we expect in the conventional checkerboard model that below  $T_N$  there would be two different types of oxygens in the basal plane. In the model of Zener polarons, on the other hand, there will be three (or even four, depending on detailed magnetic ordering) different oxygens in plane and one type between planes. However, to make a definite choice between these pictures, special, more detailed study is needed, and at the moment we can only pose this question but not answer it.

Unfortunately the spatial distribution of the Fermi-contact hyperfine fields results in a large broadening of the separate NMR lines in the spectrum measured at  $T < T_{CO}$ . It masks the anisotropy of the magnetic shift tensor and does not permit to trace the transfer of the  $2p$  spin density at oxygen in the CO PM phase, i.e., to address the orbital order more directly by studying polarization of a given  $p$  orbital.

### C. The antiferromagnetic state

Different local fields for apical oxygen in O1 and (O2/O3) sites are expected only in the spin-ordered phase below  $T_N$ . In the AF phase the AF moment canting takes place when a rather high magnetic field (7 T) is applied. The canted moment of Mn in adjacent  $ab$  planes will create at the apical oxygen an additional local field dependent on the valence state of neighboring Mn. At O1 sites the neighboring  $\text{Mn}^{3+}$  ions create a larger isotropic magnetic shift than do  $\text{Mn}^{4+}$  ions at O2/O3 sites. Indeed, as shown in Fig. 4 at  $T = 100$  K the A line splits into two lines of roughly equal intensity. A loosely packed powder sample in a strong enough external field may be considered as partially oriented with  $\mathbf{c} \parallel \mathbf{H}$ . It should be noted that the observed splitting (4 MHz) is not a result of the classic dipolar fields of the neighboring Mn ions since the difference in their effective magnetic moments is too small ( $\mu_{eff} = 2.7\mu_B$  for  $\text{Mn}^{3+}$  and  $2.2\mu_B$  for  $\text{Mn}^{4+}$  as estimated from Fig. 4 in Ref. 6).

The only slight additional broadening of the NMR spectra even around  $T_N/2$  evidences that the line shift is mainly determined by the short-range charge order and OO which have been completely formed in the CO PM phase at  $T \rightarrow T_N$ . Below 110 K it appears that the optimal rf-pulse duration increases about twofold from the low- to the high-frequency part of the A line as illustrated in Fig. 5. The same feature was found for the high-frequency spectrum when the  $B$  and  $C$  lines are resolved. This striking effect of the nonmagnetic ligand atom on the echo formation may be related to a rather strong isotropic hyperfine interaction between  $^{17}\text{O}$  nuclear spin and the Mn electron-spin system with long-range AF spin order. The detailed analysis of the spectra measured below  $T_N$  requires additional studies which are now in progress.

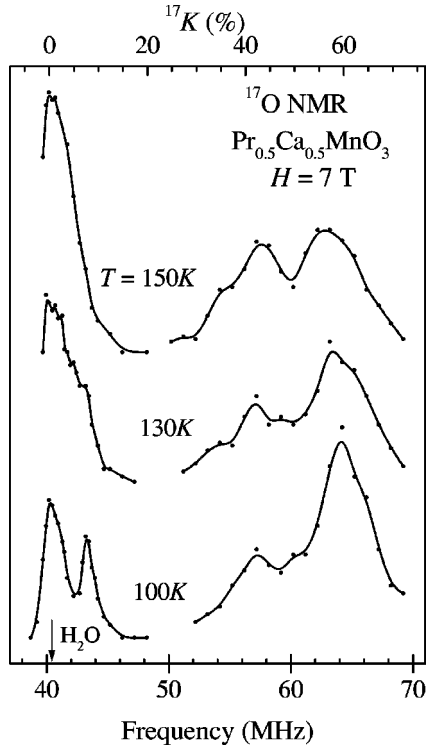


FIG. 4.  $^{17}\text{O}$  NMR spectra measured at  $H_{\text{ext}} = 7$  T in the AF phase of  $\text{Pr}_{0.5}\text{Ca}_{0.5}\text{MnO}_3$ .

#### D. Development of charge and orbital ordering

Based on the site assignment considered above we propose the following picture of the development of spin correlation in the  $\text{Pr}_{0.5}\text{Ca}_{0.5}\text{MnO}_3$  CO PM phase as seen by  $^{17}\text{O}$  NMR. In the low-temperature part of the CO PM phase the NMR spectrum represents the spin-density distribution on oxygen ions. Its value is determined not just by the Mn effective magnetic moment but, to a greater extent, by the type of spin correlations of the neighboring Mn atoms. The presence of several lines in the NMR spectrum, which can be attributed to the various oxygen sites in the lattice, shows that the corresponding spin correlations and effective magnetic moment of the neighboring cations do not change at the time scale  $t \geq 10/(\Delta\omega) \approx 10^{-6}$  s ( $\Delta\omega$  is line splitting).<sup>20</sup> The thermally activated hopping of  $e_g$  holes seems to be the main mechanism changing the charge state of the ion ( $\text{Mn}^{3+} - \text{Mn}^{4+}$ ) and the spin correlations between the neighboring ions, which results in the “melting” of OO in the CO PM phase. With increasing temperature the fine structure of the spectrum is smeared as the corresponding correlation time ( $\tau_c$ ) of the specific hopping becomes comparable with  $(\Delta\omega)^{-1}$ . As a result the various spin configurations are no more distinguishable at higher temperature.

The splitting of the NMR spectrum just below  $T_{CO}$  into the A and (B+C) lines may be explained as follows. As has been mentioned above the oxygen nuclei responsible for the A line are located between two antiferromagnetically correlated Mn ions from the adjacent *ab* plane whereas those responsible for (B+C) line have two neighboring Mn ions in the same *ab* plane. The resolution of the A line shows that just below  $T_{CO}$  the correlation time of the antiferromagnetic

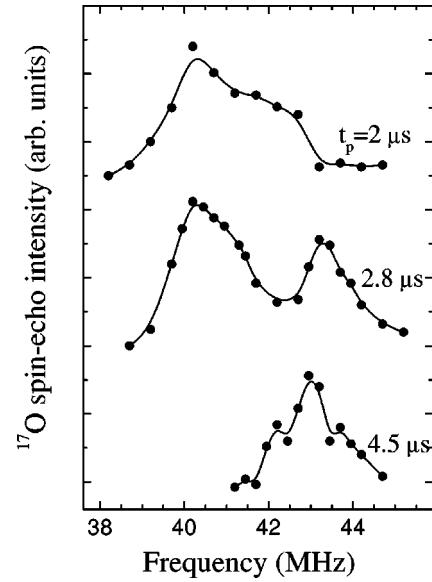


FIG. 5. Evolution of the echo-spectra shape of the A line measured with different rf-pulse durations ( $t_p$ ) at  $T = 100$  K in the AF phase.

cally correlated spin of the neighboring Mn from adjacent *ab* planes becomes long compared to the NMR time scale. By contrast, the (B+C) line is still unresolved just below  $T_{CO}$ . Thus in the first stage of the charge ordering the three-dimensional motion of  $e_g$  electrons transforms preferentially into a two-dimensional hopping within the *ab* planes. Such an ordering phase transition may be considered as the nucleation of antiferromagnetically ordered clusters which grow at the expense of the CD PM phase which dominates above  $T_{CO}$ . Furthermore as the temperature decreases and the unresolved (B+C) line is shifted toward high frequency a shoulder appears on the low-frequency part (see spectra for  $T \approx 200$  K in Fig. 2). The temperature dependence of this signal follows the same Curie-Weiss law as the peak in the CD PM phase (dashed line in Figs. 2 and 3). Its relative intensity decreases with temperature and becomes negligible only near  $T_N$ . This may indicate that almost down to  $T_N$  traces of the CD PM phase remain in the CO PM phase.

The proposed NMR interpretation of the ordering in the CO PM phase is in good agreement with the main results of the resonant x-ray<sup>4</sup> and neutron-diffraction studies.<sup>6–8</sup> It should be noted that the time scales required to get a quasi-static picture of charge distribution in NMR ( $t_{\text{nmr}} > 10^{-6}$  s) and in neutron-diffraction ( $t_{\text{nd}} \sim 10^{-12}$  s) experiments are very different. Both methods confirm the presence of FM correlations between Mn ions as dominant spin fluctuations in the CD PM phase which reduce in intensity below  $T_{CO}$ .

In the neutron-scattering experiments the short-range FM correlations are considered as static whereas they are seen still as a low-frequency dynamic phenomenon in the NMR spectra. In conclusion, the distribution of spin density and the development of the charge and orbital ordering in the paramagnetic state of  $\text{Pr}_{0.5}\text{Ca}_{0.5}\text{MnO}_3$  were studied by means of  $^{17}\text{O}$  NMR. It is shown that the main interaction of oxygen is the isotropic hyperfine Fermi-contact interaction with the

$s$ -electron spin density transferred from the nearest-neighbor Mn ions. The resulting magnetic line shift is very sensitive to both the electronic configuration of the neighboring cation ( $\text{Mn}^{+3}/\text{Mn}^{4+}$ ) and to their specific spin-pair correlations that develop on cooling in the charge- and orbital ordered PM phase. It is shown that with increasing temperature the melting of the orbital ordering first develops within the  $ab$  plane whereas the AF correlations between Mn ions in adjacent layers are more stable and disappear only when  $T$  approaches  $T_{CO}$ .

## ACKNOWLEDGMENTS

We are very grateful to Professor A. Kaul for supplying us the starting  $\text{Pr}_{0.5}\text{Ca}_{0.5}\text{MnO}_3$  material and to Dr. A. Inyushkin for  $^{17}\text{O}$  isotope enrichment. The work is supported partly by the Russian Foundation for Basic Research (Grant No. 02-02-16357a) as well as by CRDF Grant No. RP2-2355 and INTAS Grant No. 01-2008. We are especially grateful for support of A.Y. by ESPCI.

- <sup>1</sup>C. Zener, Phys. Rev. **82**, 403 (1951).
- <sup>2</sup>Z. Jirak, S. Krupicka, Z. Simsa, M. Dlouha, and Z. Vratilav, J. Magn. Magn. Mater. **53**, 153 (1985).
- <sup>3</sup>Y. Tomioka, A. Asamitsu, H. Kuwahara, Y. Morimoto, and Y. Tokura, Phys. Rev. B **53**, R1689 (1996).
- <sup>4</sup>M.v. Zimmerman, C.S. Nelson, J.P. Hill, D. Gibbs, H. Nakao, Y. Wakabayashi, Y. Murakami, Y. Tokura, Y. Tomioka, T. Arima, and C.-C. Kao, Phys. Rev. B **64**, 064411 (2001); M.v. Zimmerman, C.S. Nelson, J.P. Hill, D. Gibbs, M. Blume, D. Casa, B. Keimer, Y. Murakami, C.-C. Kao, C. Venkataraman, T. Cog, Y. Tomioka, and Y. Tokura, *ibid.* **64**, 195113 (2001).
- <sup>5</sup>S. Mori, T. Katsufuji, N. Yamamoto, C.H. Chen, and S.-W. Cheong, Phys. Rev. B **59**, 13 573 (1999).
- <sup>6</sup>Z. Jirak, F. Damay, M. Hervieu, C. Martin, B. Raveau, G. Andre, and F. Bouree, Phys. Rev. B **61**, 1181 (2000).
- <sup>7</sup>R. Kajimoto, H. Yoshizawa, Y. Tomioka, and Y. Tokura, Phys. Rev. B **63**, 212407 (2001).
- <sup>8</sup>R. Kajimoto, T. Kakeshita, Y. Oohara, H. Yoshizawa, Y. Tomioka, and Y. Tokura, Phys. Rev. B **58**, R11 837 (1998).
- <sup>9</sup>E.A. Turov and M.P. Petrov, *Nuclear Magnetic Resonance in Ferro- and Antiferromagnets* (Halsded, New York, 1972).
- <sup>10</sup>It might be noted that a rough estimate for quadrupole coupling of oxygen in  $\text{PrCaMnO}_3$  falls in the range of  $^{17}\nu_Q=(0.95-1.6)$  MHz reported for other oxides with perovskite or layered-perovskite crystal structures such as  $(\text{BaK})(\text{PbBi})\text{O}_3$  [E. Oldfield, Ch. Coretsopoulos, S. Yang, L. Reven, H.Ch. Lee, J. Shore, O.H. Han, E. Ramli, and D. Hinks, Phys. Rev. B **40**, 6832 (1989); Yu. Piskunov, A. Gerashenko, A. Pogudin, A. Ananyev, K. Mikhalev, K. Okulova, S. Verkhbovskii, A. Yakubovsky, and A. Trokiner, *ibid.* **65**, 134518 (2002)]; and  $\text{YBaCuO}$  [M. Taki-gawa *et al.* Phys. Rev. Lett. **63**, 1865 (1989)].
- <sup>11</sup>Y. Yoshinari, P.C. Hammel, J.D. Thompson, and S.-W. Cheong, Phys. Rev. B **60**, 9275 (1999).
- <sup>12</sup>D.E. O'Reilly and T. Tsang, J. Chem. Phys. **40**, 734 (1963).
- <sup>13</sup>S. Fraga, J. Karwowski, and K.M.S. Saxena, *Handbook of Atomic Data* (Elsevier Scientific, Amsterdam, 1976).
- <sup>14</sup>R.J. Shulman and V. Jaccarino, Phys. Rev. **108**, 1219 (1957).
- <sup>15</sup>I.S. Elfimov (private communication).
- <sup>16</sup>M. Karplus and G.K. Fraenkel, J. Chem. Phys. **35**, 1312 (1961).
- <sup>17</sup>R.E. Watson and A.J. Freeman, Phys. Rev. **134**, A1526 (1964).
- <sup>18</sup>R.E. Watson and A.J. Freeman, in *Hyperfine Interactions*, edited by A.J. Freeman and R.B. Frankel (Academic, New York, 1967), p. 345.
- <sup>19</sup>V.I. Anisimov, I.S. Elfimov, M.A. Korotin, and K. Terakura, Phys. Rev. B **55**, 15 494 (1997).
- <sup>20</sup>A. Abragam, *The Principles of Nuclear Magnetism* (Clarendon, Oxford, 1961).
- <sup>21</sup>A. Daoud-Aladine, J. Rodriguez-Carvajal, L. Pinsard-Gaudart, M.T. Fernandez-Diaz, and A. Revcolevschi, Phys. Rev. Lett. **89**, 097205 (2002).
- <sup>22</sup>F. Damay, Z. Jirák, M. Hervieu, C. Martin, A. Maignan, B. Raveau, G. André, and F. Bourée, J. Magn. Magn. Mater. **190**, 221 (1998).
- <sup>23</sup>Ch. Renner, G. Aeppli, B.-G. Kim, Yeong-Ah Soh, and S.-W. Cheong, Nature (London) **416**, 518 (2002).